

# MEASUREMENTS OF FOREST BIOMASS CHANGE USING L- AND P-BAND SAR BACKSCATTER

*Ivan Huuva, Johan E. S. Fransson, Henrik J. Persson, Jörgen Wallerman*  
Swedish University of Agricultural Sciences  
Dept. of Forest Resource Management  
SE-901 83 Umeå, Sweden

*Lars M. H. Ulander, Erik Blomberg, Maciej J. Soja*  
Chalmers University of Technology  
Dept. of Space, Earth and Environment  
Gothenburg, Sweden

## ABSTRACT

Three-year forest above-ground biomass change were measured using L- and P-band Synthetic Aperture Radar (SAR) backscatter. The SAR data were collected in the airborne BioSAR 2007 and BioSAR 2010 campaigns over the hemiboreal Remningstorp test site in southern Sweden. Regression models for biomass were developed using reference biomass maps created using airborne laser scanning data and field measurements.

The results from regression analysis show that using HV backscatter (or VH) in a model with above-ground biomass and backscatter change on either natural logarithmic or square root, and decibel scale, respectively, explained most of the variation in the biomass change, both for L- and P-band. In the case of L-band, the two best cases showed  $R^2$  values of 66%, when comparing two SAR images acquired 2007 and 2010. For P-band using the same models, the best cases showed  $R^2$  values of 62%. In summary, the results look promising using L- and P-band backscattering for mapping biomass change.

**Index Terms**— Biomass, forestry, L-band, P-band, radar, modeling

## 1. INTRODUCTION

Global warming is caused by the elevated concentrations of greenhouse gases into the atmosphere. The most prominent of these gases is carbon dioxide [1]. The biosphere acts as net carbon sink, and changes in its efficiency in storing carbon need to be better understood [2]. Forests are a large part of terrestrial biosphere and their carbon storage capacity of forests is proportional to the biomass they contain. This necessitates large-scale mapping of forest biomass. Images from Synthetic Aperture Radar (SAR) systems have the benefit of being insensitive to weather and lighting

conditions, making it easy to reliably get useful full coverage data even over large areas. Furthermore, relatively long wavelength of SAR systems is an advantage, as it can penetrate the canopy, and thus allows for retrieval of above-ground biomass. Previous studies have used both L- and P-band SAR data to retrieve biomass in boreal and hemiboreal forests [3, 4], and L-band data have also been used to detect clear-cuts and storm damages [5, 6], but estimation of biomass change from growth using L-band data in hemiboreal forests has not, to the knowledge of the authors, been studied.

The objective of this study is to investigate the potential of estimating changes in above-ground biomass using airborne L- and P-band SAR data from the BioSAR 2007 and BioSAR 2010 campaigns over the hemiboreal test site in Remningstorp in southern Sweden. Specifically, regression models for biomass change were developed and evaluated for L- and P-band SAR data.

## 2. TEST SITE AND DATA

The study used SAR data, *in situ* data, and airborne laser scanning data collected in the airborne campaigns BioSAR 2007 and BioSAR 2010. Full descriptions of the campaigns and the data can be found in the final reports [7, 8]. The data were collected in the Remningstorp test site in southern Sweden (58°30' N, 13°40' E). The site consists of managed forest dominated by Norway spruce (*Picea abies*) and Scots pine (*Pinus sylvestris*) with some birch (*Betula* spp.). The ground slopes on the site are generally small, with elevations between 120 m and 145 m above sea level.

### 2.1. SAR data

The SAR images used are fully polarimetric in L- and P-band. For 2007, the SAR data were collected using the German E-SAR system by the German Aerospace Center (DLR), while

the 2010 SAR data were collected using the French SETHI system by ONERA. The two systems, and hence the SAR data for the two years are not identical.

The 2007 SAR data, from E-SAR, were delivered with a center frequency of 1300 MHz and a bandwidth of 94 MHz for L-band, and a center frequency of 350 MHz and a bandwidth of 70 MHz for P-band (Table I).

The 2010 SAR data, from SETHI, were collected with a center frequency of 1325 MHz and a bandwidth of 150 MHz for L-band, and a center frequency of 360 MHz and a bandwidth of 166 MHz for P-band, with some notches and gaps to avoid radio frequency interference (Table II).

TABLE I  
List of E-SAR datasets

Scene id	Band	Flight track heading	Acquisition data
104	L	200°	9 March 2007
205	L	200°	31 March 2007
405	L	200°	2 May 2007
109	P	200°	9 March 2007
306	P	200°	2 April 2007
411	P	200°	2 May 2007

TABLE II  
List of SETHI datasets

Scene id	Band	Flight track heading	Acquisition data
1	L	200°	23 Sept. 2010
2	L	200°	23 Sept. 2010
5	L	179°	23 Sept. 2010
1	P	200°	23 Sept. 2010
2	P	200°	23 Sept. 2010
5	P	179°	23 Sept. 2010

Each pixel in the full resolution images is calibrated to the average radar cross-section per unit ground area, after which a first order correction for variations in incidence angle is applied, to obtain what in the henceforth will be referred to simply as the backscatter. The resulting full resolution backscatter images are then downsampled to a pixel size of 50 m × 50 m in order to create backscatter maps that match the created biomass maps.

## 2.2. *In situ* data

The *in situ* data consisted of two 10 m radius field plot grids. One of the two plot grids has a plot spacing of 40 m, and was surveyed in 2004–2005. This grid was used for estimating the true biomass in 2007. The other plot grid has a spacing of 200 m, was surveyed in 2010, and was used in this study to estimate the true biomass in 2010.

Since the field plot grids for the two years were not the same, and the plot overlap is small, changes in biomass could not be directly measured *in situ* with a reasonable amount of data points. Instead, biomass maps were created for each year

using the grid of plots and data from the airborne laser scanning from that year. The biomass maps are further described in 2.3. The difference between these biomass maps and the difference in backscatter between pairs of SAR images at each 50 m × 50 m pixel are used in the regression analysis.

## 2.3. Biomass maps

As previously mentioned, the field data used for the two years were not from the same plots, necessitating an indirect approach to retrieve the biomass change from 2007 and 2010. To this end, biomass maps were created. As mentioned, airborne laser scanning was also conducted at the test site for each year. Metrics from the resulting point clouds were used together with the *in situ* data to produce an above-ground biomass map for both years.

## 3. METHOD

To investigate the potential of L- and P-band backscatter for mapping the change of above-ground biomass the following set of regression models were applied at the 50 m × 50 m pixels:

$$AGB_{2010} - AGB_{2007} = \beta_0 + \beta_1(\gamma_{2010}^\circ - \gamma_{2007}^\circ) + \varepsilon \quad (1)$$

$$AGB_{2010} - AGB_{2007} = \beta_0 + \beta_1(\sqrt{\gamma_{2010}^\circ} - \sqrt{\gamma_{2007}^\circ}) + \varepsilon \quad (2)$$

$$AGB_{2010} - AGB_{2007} = \beta_0 + \beta_1 10 \cdot \log_{10}\left(\frac{\gamma_{2010}^\circ}{\gamma_{2007}^\circ}\right) + \varepsilon \quad (3)$$

$$\sqrt{AGB_{2010}} - \sqrt{AGB_{2007}} = \beta_0 + \beta_1(\gamma_{2010}^\circ - \gamma_{2007}^\circ) + \varepsilon \quad (4)$$

$$\sqrt{AGB_{2010}} - \sqrt{AGB_{2007}} = \beta_0 + \beta_1(\sqrt{\gamma_{2010}^\circ} - \sqrt{\gamma_{2007}^\circ}) + \varepsilon \quad (5)$$

$$\sqrt{AGB_{2010}} - \sqrt{AGB_{2007}} = \beta_0 + \beta_1 10 \cdot \log_{10}\left(\frac{\gamma_{2010}^\circ}{\gamma_{2007}^\circ}\right) + \varepsilon \quad (6)$$

$$\ln\left(\frac{AGB_{2010}}{AGB_{2007}}\right) = \beta_0 + \beta_1(\gamma_{2010}^\circ - \gamma_{2007}^\circ) + \varepsilon \quad (7)$$

$$\ln\left(\frac{AGB_{2010}}{AGB_{2007}}\right) = \beta_0 + \beta_1(\sqrt{\gamma_{2010}^\circ} - \sqrt{\gamma_{2007}^\circ}) + \varepsilon \quad (8)$$

$$\ln\left(\frac{AGB_{2010}}{AGB_{2007}}\right) = \beta_0 + \beta_1 10 \cdot \log_{10}\left(\frac{\gamma_{2010}^\circ}{\gamma_{2007}^\circ}\right) + \varepsilon \quad (9)$$

where  $AGB_{2010} - AGB_{2007}$ ,  $\sqrt{AGB_{2010}} - \sqrt{AGB_{2007}}$ , and  $\ln(AGB_{2010}/AGB_{2007})$  are the above-ground biomass change on linear, square root, and natural logarithmic scale, respectively,  $\gamma_{2010}^\circ$  and  $\gamma_{2007}^\circ$  is the backscatter from a given SAR system (E-SAR or SETHI) and polarization (HH, HV, VH and VV) for year 2010 and 2007, respectively,  $\beta_0$  and  $\beta_1$  are the regression coefficients, and  $\varepsilon$  is the random error for the true biomass. The backscatter change measures were not mixed in the same model, i.e. only one polarization were used for each model.

#### 4. RESULTS

The main results from the regression modeling of the above-ground biomass change are shown in Table II. The strongest dependence between above-ground biomass change and backscatter change is observed for L-band HV (or VH), while for HH and VV the dependence is weaker. For both L- and P-band, in all polarizations, the biomass change is offset relative to zero backscatter change (see Figs. 1 and 2 for HV).

TABLE II  
Results from the regression modeling of above-ground biomass change using the models (1) – (9) (best cases for L- and P-band)

Eq.	Scene id	Band	Polarization	R <sup>2</sup> (%)
(1)	0405 – 05	L	VH	54
(1)	0306 – 05	P	HH	49
(2)	0205 – 05	L	HV	59
(2)	0306 – 05	P	HV	56
(3)	0104 – 05	L	HV	62
(3)	0306 – 05	P	HV	60
(4)	0405 – 05	L	VH	56
(4)	0306 – 05	P	HH	48
(5)	0405 – 05	L	VH	62
(5)	0109 – 05	P	HV	57
(6)	0205 – 05	L	HV	66
(6)	0109 – 05	P	VH	62
(7)	0405 – 05	L	HV	53
(7)	0306 – 05	P	HH	45
(8)	0405 – 05	L	HV	61
(8)	0109 – 05	P	HV	55
(9)	0104 – 05	L	HV	66
(9)	0109 – 05	P	HV	62

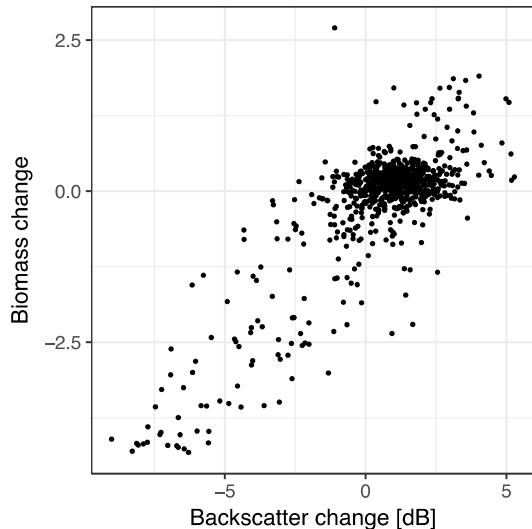


Fig. 1. Scatterplot of above-ground biomass and L-band HV backscatter change on natural logarithmic and decibel scale, respectively, based on biomass and backscatter maps with a cell size of 50 m × 50 m (best case corresponding to Eq. (9) in Table II). A positive change means that the observation from 2010 was higher than that from 2007.

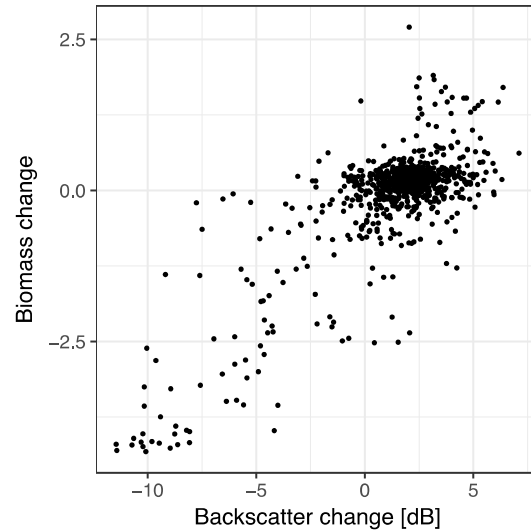


Fig. 2. Scatterplot of above-ground biomass and P-band HV backscatter change on natural logarithmic and decibel scale, respectively, based on biomass and backscatter maps with a cell size of 50 m × 50 m (best case corresponding to Eq. (9) in Table II). A positive change means that the observation from 2010 was higher than that from 2007.

#### 5. DISCUSSION

In this study, above-ground biomass change has been investigated using L- and P-band data from the E-SAR (2007) and SETHI (2010) SAR systems at a test site with hemiboreal forest in southern Sweden. The results from regression analysis show that using HV backscatter (or VH) in a model with above-ground biomass and backscatter change on either natural logarithmic or square root, and decibel scale, respectively, explained most of the variation in the biomass change, both for L- and P-band (see Eqs. (6) and (9)). In the case of L-band, the two best cases showed R<sup>2</sup> values of 66%, when comparing the two SAR images with the scene ids 0205 – 05 and 0104 – 05. For P-band using the same models, the best cases showed R<sup>2</sup> values of 62% using the SAR images with the same scene ids 0109 – 05. Note that the images giving the best results for both L- and P-band in all cases have different flight headings, i.e. 200° and 179°.

The intensity of backscatter is not only dependent on the amount of biomass at a certain position, but varies significantly with other variables such as soil, stem, and canopy moisture, and forest structure variables such as tree species, number of stems, and spatial distribution of trees. The moisture can vary significantly over both seasons and even days, making it especially challenging when estimating biomass change. To mitigate the effect of soil moisture and calibration errors a backscatter change offset correction method (used for P-band data) were proposed in [9]. This

correction method will be applied and evaluated also on L-band data in future studies. The correction is based on the HH-VV backscatter ratio, found to be relatively insensitive to moisture, and aims to correct the backscatter maps so that areas with very small changes in biomass correspond to areas with very small changes in backscatter. Furthermore, to improve the modeling of above-ground biomass change, models with backscatter from a combination of different polarizations (and transformations thereof) as independent variables will be investigated.

## 6. REFERENCES

- [1] T. F. Stocker, D. Qin, G-K. Plattner, M Tignor, S. K. Allen, J. Boschung, A. Nauels, Y. Xia, V. Bex, and P. M. Midgley, "Climate change 2013: The physical science basis," Tech. Rep., Intergovernmental Panel on Climate Change, 2013, IPCC Fifth Assessment Report.
- [2] J. G. Canadell, C. Le Quéré, M. R. Raupach, C. B. Field, E. T. Buitenhuis, P. Ciais, T. J. Conway, N. P. Gillett, R. A. Houghton, and G. Marland, "Contributions to accelerating atmospheric CO<sub>2</sub> growth from economic activity, carbon intensity, and efficiency of natural sinks," Proceedings of the National Academy of Sciences, vol. 104, no. 47, pp. 18866–18870, Nov. 2007.
- [3] G. Sandberg, L.M.H. Ulander, J.E.S. Fransson, J. Holmgren, and T. Le Toan, "L- and P-band backscatter intensity for biomass retrieval in hemiboreal forest," Remote Sensing of Environment, vol. 115, no. 11, pp. 2874–2886, 2011.
- [4] M. Neumann, S. S. Saatchi, L. M. H. Ulander, and J. E. S. Fransson, "Assessing performance of L- and P-band polarimetric interferometric SAR data in estimating boreal forest above-ground biomass," IEEE Transactions on Geoscience and Remote Sensing, vol. 50, no. 3, pp. 714–726, March 2012.
- [5] M. Santoro, A. Pantze, J. E. S. Fransson, J. Dahlgren, and A. Persson, "Nation-wide clear-cut mapping in Sweden using ALOS PALSAR strip images," Remote Sensing, vol. 4, no. 6, pp. 1693–1715, 2012.
- [6] J. E. S. Fransson, M. Magnusson, H. Olsson, L. E. B. Eriksson, G. Sandberg, G. Smith-Jonforsen, and L. M. H. Ulander, "Detection of forest changes using ALOS PALSAR satellite images," Proceedings of IGARSS 2007, Sensing and Understanding Our Planet, Barcelona, Spain, 23-27 July, 2007, pp. 2330-2333.
- [7] I. Hajnsek, R. Scheiber, L. M. H. Ulander, A. Gustavsson, G. Sandberg, S. Tebaldini, A. M. Guarnieri, F. Rocca, F. Bombardini, and M. Pardini, "BioSAR 2007, Technical assistance for the development of airborne SAR and geophysical measurements during the BioSAR 2007 experiment: Final report without synthesis," Tech. Rep., European Space Agency, 2008, ESA Contract No.: 20755/07/NL/CB.
- [8] L. M. H. Ulander, A. Gustavsson, B. Flood, D. Murdin, P. Dubois-Fernandez, X. Dupuis, G. Sandberg, M. J. Soja, L. E. B. Eriksson, J. E. S. Fransson, J. Holmgren, and J. Wallerman, "BioSAR 2010, Technical assistance for the development of airborne SAR and geophysical measurements during the BioSAR 2010 experiment: Final report," Tech. Rep., European Space Agency, 2011, ESA Contract No.: 4000102285/10/NL/JA/ef.
- [9] G. Sandberg, L. M. H. Ulander, J. Wallerman, and J. E. S. Fransson, "Measurements of forest biomass change using P-band SAR backscatter," IEEE Transactions on Geoscience and Remote Sensing, vol. 52, no. 10, pp. 6047–6061, Oct. 2014.